Journal of Environmental Management 358 (2024) 120908

Contents lists available at ScienceDirect

Journal of Environmental Management

journal homepage: www.elsevier.com/locate/jenvman

Research article

Enhancing nitrogen removal in the partial denitrification/anammox processes for SO_4^- - Rich wastewater treatment: Insights into autotrophic and mixotrophic strategies

Dominika Derwis [a], Hussein E. Al-Hazmi [a,**], Joanna Majtacz [a], Sławomir Ciesielski [b], Jacek Mąkinia [a,*]

[a] Department of Sanitary Engineering, Faculty of Civil and Environmental Engineering, Gdańsk University of Technology, 11/12 Narutowicza Street, 80-233, Gdańsk, Poland

[b] Department of Environmental Biotechnology, Faculty of Geoengineering, University of Warmia and Mazury in Olsztyn, Słoneczna 45G, Olsztyn, 10-719, Poland

ARTICLE INFO

Keywords:
Anammox
Mixotrophic denitrification
Sulfur-dependent autotrophic denitrification
Nitrogen removal performance
Microbial interaction

ABSTRACT

The investigation of partial denitrification/anammox (PD/anammox) processes was conducted under autotrophic (N–S cycle) and mixotrophic (N–S–C cycle) conditions over 180 days. Key findings revealed the remarkable capability of SO_4^{2-}-dependent systems to produce NO_2^- effectively, supporting anaerobic NH_4^+ oxidation. Additionally, SO_4^{2-} served as an additional electron acceptor in sulfate reduction ammonium oxidation (SRAO). Increasing influent SO_4^{2-} concentrations notably improved ammonia utilization rates (AUR) and NH_4^+ and total nitrogen (TN) utilization efficiencies, peaking at 57% for SBR1 and nearly 100% for SBR2. Stoichiometric analysis showed a 7.5-fold increase in AUR (SRAO and anammox) in SBR1 following SO_4^{2-} supplementation. However, the analysis for SBR2 indicated a shift towards SRAO and mixotrophic denitrification, with anammox disappearing entirely by the end of the study. Comparative assessments between SBR1 and SBR2 emphasized the impact of organic compounds (CH_3COONa) on transformations within the N–S–C cycle. SBR1 performance primarily involved anammox, SRAO and other SO_4^{2-} utilization pathways, with minimal S-dependent autotrophic denitrification (SDAD) involvement. In contrast, SBR2 performance encompassed SRAO, mixotrophic denitrification, and other pathways for SO_4^{2-} production. The SRAO process involved two dominant genera, such as *Candidatus* Brocadia and PHOS-HE36.

1. Introduction

Conventional nitrification-denitrification is the most common method of nitrogen (N) removal in municipal wastewater treatment plants (WWTPs). Despite a high utilization efficiency of the process, its sustainability has been questioned due to high energy demand, carbon (C) supplementation and potential for significant nitrous oxide (N_2O) emissions (Zhou et al., 2020). An alternative approach to N removal, based on anaerobic ammonia (NH_4^+) oxidation (anammox), can overcome these disadvantages. This process converts NH_4^+ into nitrogen gas (N_2), using nitrite (NO_2^-) as an electron acceptor (Zekker et al., 2015, 2023). However, anammox is challenged by a stable supply of NO_2^- to ensure the optimum ratio of NH_4^+/NO_2^-. Partial nitritation (PN) was initially proposed as sole solution, but the competition from nitrite-oxidizing bacteria (NOB) for NO_2^- can reduce the overall N utilization efficiency in anammox-based systems (Wu et al., 2022). More recently, partial denitrification (PD), involving reduction of nitrate (NO_3^-) to NO_2^-, has emerged as a promising alternative pathway of generating NO_2^- for anammox (Al-Hazmi et al., 2023). The advantages of PD include reduced energy demand and reduced N_2O emissions with a small need for supplemental C.

Exploring denitrification processes in wastewater treatment requires a thorough understanding the dynamic interactions between heterotrophic and autotrophic mechanisms. Heterotrophic denitrification is predominantly carried out by bacteria utilizing organic C as their energy source. In contrast to the utilization of organic substances, autotrophic

* Corresponding author.
** Corresponding author.
E-mail addresses: dominika.derwis@pg.edu.pl (D. Derwis), hussein.hazmi1@pg.edu.pl (H.E. Al-Hazmi), joamajta@pg.edu.pl (J. Majtacz), slavcm@uwm.edu.pl (S. Ciesielski), jmakinia@pg.edu.pl (J. Mąkinia).

https://doi.org/10.1016/j.jenvman.2024.120908
Received 1 February 2024; Received in revised form 28 March 2024; Accepted 12 April 2024

denitrification involves the use of inorganic compounds such as hydrogen (H_2), sulfide (S^{2-}), elemental sulfur (S^0), thiosulfate ($S_2O_3^{2-}$), iron (Fe^{2+}), and manganese (Mn^{2+}) as electron donors (Zhang et al., 2022). This innovative approach to denitrification relies on non-organic sources to supply electrons for the reduction of N compounds.

One notable denitrification process that utilizes sulfur (S) compounds (S^{2-}, S^0, and $S_2O_3^{2-}$) as electron donors is S-dependent autotrophic denitrification (SDAD) (Grubba et al., 2022). Although the N utilization rate of SDAD is lower compared to heterotrophic denitrification (Qian et al., 2018), the advantages of SDAD comprise low sludge production and no need for external C (Cao et al., 2019; Di Capua et al., 2019) as well as lower N_2O emissions (Huang et al., 2019).

Nevertheless, the reduced forms of S may not always be present in wastewater, except for SO_4^{2-}. The resolution to this issue involves either executing the autotrophic sulfate reduction ammonium oxidation (SRAO) process, which reduces SO_4^{2-} to reduced S forms, or opting for the second solution, which entails the heterotrophic reduction of SO_4^{2-} by sulfate-reducing bacteria (SRB) before initiating S-dependent PD. Moreover, SRAO can also be a source of NO_2^- for the anammox reaction (Grubba et al., 2022).

Wastewater streams frequently exhibit complexity, comprising a blend of N, S and C compounds. This is evident in scenarios, such as landfill leachates or industrial wastewater originating from mining operations or paper production (Ma et al., 2022b). Consequently, wastewater seldom aligns exclusively with either heterotrophic or autotrophic conditions. To address this complexity, extensive research has focused on combining autotrophic and heterotrophic denitrification in mixotrophic systems (Huang et al., 2022). These systems enable the coexistence of autotrophic and heterotrophic organisms, which can lead to improving the stability and overall N removal performance of wastewater treatment systems. Mixotrophic systems facilitate the simultaneous removal of N, S and C, thereby reducing the need for supplementary organic electron donors (Xu et al., 2015).

This study addresses a critical research gap by examining the integration of partial S-dependent denitrification (N–S cycle in SBR1) or mixotrophic denitrification with the anammox process (N–S–C cycle in SBR2) in a single reactor for wastewater treatment, particularly focusing on streams rich in NH_4^+, NO_3^-, SO_4^{2-}, and COD. Additionally, our objective was to utilize the SRAO process to reduce SO_4^{2-} to its reduced forms for SDAD, a novel approach not previously investigated in literature. Expanding upon our previous research in the same SBRs configurations, which demonstrated the positive effects of SO_4^{2-} supplementation on NH_4^+ and SO_4^{2-} utilization rates (AUR and SUR) in both autotrophic (Derwis et al., 2023) and mixotrophic conditions (Derwis et al., 2024), we now investigate the combined impact of SO_4^{2-} supplementation and the integration of the N–S (SBR1) or N–S–C (SBR2) cycles on PD/anammox performance. An innovative aspect of this study is the absence of NO_2^- in the influent, which was present in both previous studies.

The primary objective of this study was to operate two parallel SBRs for evaluating and comparing the performance of S-dependent denitrification (SBR1) versus mixotrophic denitrification (SBR2) processes alongside anammox, with and without COD supplementation. It was hypothesized that integrating autotrophic (N–S) and mixotrophic (N–S–C) processes could generate sufficient amounts of NO_2^- to effectively support anammox, while the SRAO process would enhance NH_4^+ utilization. Furthermore, a positive influence of additional SO_4^{2-} on N–S compounds removal under autotrophic conditions in SBR1 and N–S–C compounds under mixotrophic conditions in SBR2 was expected. Moreover, the production of reduced S compounds for SDAD would occur through SO_4^{2-} reduction in SRAO (N–S) and additionally by SRB (N–S–C). In addition to evaluating process performance, the contributions of individual metabolic pathways and microbial communities in the reactors were elucidated. By integrating stoichiometric reactions with observed behavior of N compounds (NH_4^+, NO_2^-, NO_3^-), SO_4^{2-}, and COD, a comprehensive understanding of integrated N–S and N–S–C metabolism was sought. Furthermore, key functional bacterial groups necessary for these processes were identified. The results of this study have significant implications for wastewater treatment practices, offering insights into optimizing PD/anammox processes for S-rich streams. By emphasizing the innovative aspects of the proposed approach and clearly defining the hypotheses and research objectives, a contribution was made to the advancement of both scientific knowledge and practical applications in environmental engineering. The study emphasizes the importance of ensuring mixotrophic conditions and obtaining reduced S compounds from SO_4^{2-} while treating the complex real wastewater, including that from various industrial sources like chemical plants, petroleum refineries, dyeing plants, tanneries, paper mills, molasses wineries, food processing plants, landfills and mining plants (Li and Tabassum, 2022).

2. Materials and methods

2.1. Laboratory setup

The laboratory setup comprised two SBRs, each with a working volume of 15 L, connected to a control box for regulating the influent/effluent flowrates and mixing. These reactors were constructed from plexiglass and placed in a water jacket to control the process temperature. A Julabo F32 (Germany) water bath was employed to achieve a precise temperature control with an accuracy of ±0.1 °C. Additionally, both reactors were equipped with a variable-speed Heidolph RZR 2041 (Germany) mechanical stirrer. For monitoring, Endress + Hauser (Switzerland) probes were employed to measure pH (EH CPS 471D-7211) and dissolved oxygen (DO) (COS22D-10P3/O) were installed and connected to two Hach Lange HQ40D (Switzerland) multimeters. Further details on the setup design and operational methodology can be found in Al-Hazmi et al. (2020). A diagram of the reactor setup is presented in the Supplementary Material (Fig. S1). To ensure data quality control, consistent measurement practices were employed, incorporating routine calibration of probes and the maintenance of uniform operating conditions.

2.2. Inoculum biomass and operational conditions

The inoculum biomass (30 L), used in the experiments, was obtained from a sidestream granular deammonification system at a large municipal wastewater treatment plant (200,000 PE) in Słupsk, Poland. The seed sludge used had a mixed liquor suspended solids (MLSS) concentration of 4500 mg/L.

Throughout a 180-day period, the reactors were consistently operated at a constant process temperature of 30 ± 1 °C without aeration. The measured DO concentration was maintained below 0.02 mg O_2/L. pH levels were controlled within the range of 7.5–7.8 by the automated addition of 6M hydrochloric acid (HCl). The synthetic medium supplied to the SBRs contained microelements based on the composition outlined in a previous study by Al-Hazmi et al. (2020). Key feed components, such as NO_3^-, NH_4^+, COD, and SO_4^{2-}, were introduced in the form of KNO_3, NH_4Cl, CH_3COONa, and $MgSO_4$, respectively.

The dynamic behavior of influent and initial concentrations in the reaction phase in both bioreactors, including NH_4^+, NO_3^-, COD and SO_4^{2-}, are illustrated in Supplementary Material (Fig. S2, Fig. S3). Influent flow rates in SBR1 and SBR2 are illustrated in Fig. S2e. NH_4^+, NO_3^-, and SO_4^{2-} were introduced into both reactors, while COD was specifically added to SBR2 to facilitate a comparison between N–S cycle (SBR1) and N–S–C (SBR2) conditions.

Influent NH_4^+ concentrations varied between 10 and 50 mg N/L, and 20–40 mg N/L for SBR1 and SBR2, respectively. Simultaneously, NO_3^- concentrations ranged from 0 to 20 mg N/L for SBR1 and 10–40 mg N/L for SBR2. Variations in NH_4^+ and NO_3^- concentrations were observed due to the accumulation of these compounds during the process, prompting periodic adjustments in dosage. Influent SO_4^{2-} concentration was kept the same in both reactors and ranged from 150 to 800 mg S/L. The

experiment comprised two stages: the first stage conducted before elevating the influent SO_4^{2-} concentration, followed by the subsequent stage after the concentration increase. The transition occurred around day 100. During the first stage, the maximum influent SO_4^{2-} concentration reached 300 mg S/L, while in the second stage, it rose to 800 mg S/L. SO_4^{2-} was introduced to simulate a SO_4^{2-}-rich wastewater scenario, anticipating its reduction to reduced S forms (S^{2-}, S^0, and $S_2O_3^{2-}$) in SRAO (N–S) and even by SRB (N–S–C). In SBR2, the influent COD concentration ranged from 100 to 200 mg COD/L, maintaining the initial higher concentration, but ultimately remaining at 100 mg COD/L for most of the period.

2.3. Microbiological and chemical analytical methods

DNA extraction from soil samples utilized the FastDNA Spin kit for soil (MP Biomedicals, USA). After thawing at room temperature, 200 mg of semi-dry biomass was bead-beaten in an Uniequip device for 5 min. The extraction, conducted in duplicates, underwent agarose gel electrophoresis for DNA quality and Quant-iT BR DNA Assay (Thermo Fisher Scientific, USA) for concentration measurement.

Taxonomic composition was determined via Illumina sequencing of the 16S rRNA gene V3–V4 regions. Raw reads were processed using Cutadapt and dada2 in QIIME2. Taxonomic assignments were made against the Silva (138 release) 16S rRNA reference database. Further analysis on EzBioCloud included computing Operational Taxonomic Units (OTU) numbers, rarefaction curves, and the Shannon alpha-diversity index. Good's coverage is calculated as 1 minus the ratio of singleton OTUs (F1) to the total sum of counts for all Operational Taxonomic Units (OTUs), where F1 represents the number of OTUs that are uniquely represented by a single sequence, and N is the cumulative count of all OTUs in the sample. Statistical significance was assessed with the Wilcoxon rank-sum test. Phylogenetic distances utilized generalized UniFrac distances, and PERMANOVA assessed genetic distance significance.

Mixed liquor samples were promptly filtered using disposable glass microfiber filters (1.2 μm) MFV-3 (47 mm diameter) sourced from Sartorius (Germany). Concentrations of NO_3^-, NO_2^-, NH_4^+, COD, and SO_4^{2-} were assessed using the DR 3900 spectrophotometer, employing dedicated cuvette tests from Hach Lange GmbH (Dusseldorf, Germany). Table S1 in Supplementary Material contains methods numbers according to Hach-Lange standards. We selected particular analysis days to encompass a crucial observation window and align with our prior investigations. The absence of sample testing and analysis between days 44–94 was attributed to operational issues with the system. Determination of MLSS and MLVSS concentrations was performed according to the Standard Method 2540 G as per the American Public Health Association (APHA) (Greenberg et al., 2005).

Cuvette measurements underwent vigilant monitoring for deviations, and if required, measurements were repeated to uphold precision. Additionally, certified cuvette tests were employed, providing certificates that encompass standard deviation, coefficient of variation, and the correlation between nominal and actual values. The standard deviation for each measured and calculated value can be found in the Supplementary Material (Table S2).

2.4. Determination of specific process rates based on stoichiometric calculations

The determination of specific process utilization/production rates was based on the maximum slopes of several variables, including NH_4^+ utilization rate (AUR), NO_3^- production/utilization rate (NPR/NUR), COD utilization rate (CUR), and SO_4^{2-} production/utilization rate$^-$ (SPR/SUR). All calculated process rates underwent rigorous statistical analysis and were subjected to N–S–C mass balances (Table S3). Furthermore, the efficiency of N, SO_4^{2-}, and COD utilization was determined by assessing the differences between influent and effluent concentrations, where negative values denoted the production of SO_4^{2-}.

The stoichiometric analysis was carried using the SOLVER tool in MS Excel assuming the same reaction stoichiometries as described in Derwis et al. (2024). The stoichiometric calculations were performed based on reactions described in the literature (Fdz-Polanco et al., 2001; Huang et al., 2019; Sun et al., 2018). This series of reaction equations facilitated the dissection of total rates, attributing them to specific processes, guided by the following assumptions.

1. Anammox, SDAD, SRAO, and SO_4^{2-} utilization other than SRAO (SUR_other) were considered in SBR1,
2. Anammox, mixotrophic denitrification, SRAO, heterotrophic SO_4^{2-} reduction, other SO_4^{2-} utilization (SUR_other) and other SO_4^{2-} production (SPR_other) were considered in SBR2,
3. Other SO_4^{2-} production (SPR_other) and utilization (SUR_other) processes operate independently of the N cycle. SPR_other could involve the oxidation of reduced S species using trace oxygen, while SUR_other might include SO_4^{2-} utilization using bacterially produced organic matter.

Analyses were conducted on the days when microbiological sampling took place (1d, 94d, 114d, 164d) to assess patterns in process rates and variations in microbial composition. The selected analysis periods corresponded to key stages in the study: at the outset (1d), prior to heightened SO_4^{2-} addition in both reactors (94d), immediately following the increase in SO_4^{2-} addition (114d), and finally, at the end of the study (164d). This strategic selection facilitated a comprehensive examination of microbial structural changes in response to varying conditions over the study duration. The outcomes were visualized through Sankey diagrams created in the simulation platform GPS-X ver. 7.0 (Hydromantis, Canada).

3. Results

3.1. Sulfate-dependent anaerobic ammonium oxidation indicators (AUR, SPR/SUR)

During the study period, MLSS concentrations varied from 3000 to 3300 mg/L, while the volatile fraction (MLVSS) concentrations ranged from 2300 to 2500 mg/L, representing approximately 76% of MLSS.

The dynamics of AUR and SPR/SUR throughout the entire study period are presented in Fig. 1. Initially, in both reactors, the AUR was at low values of 0.5–2 mg N/(g VSS • h) until day 118 in SBR1, and 1.1–2 mg N/(g VSS • h) until day 103 in SBR2. Following the initial period, a significant increase in AUR to a maximum value of 6.1 mg N/(g VSS • h) on day 180 and 4.8 mg N/(g VSS • h) on day 148 was observed in SBR1 and SBR2, respectively. After 100 days, the SO_4^{2-} supplementation began to increase, coinciding with the rising AUR in both reactors (Fig. 1a–b).

In contrast, SO_4^{2-} was utilized in SBR1 with a gradual increase in the SUR from 1.6 mg S/(g VSS • h) to 12.7 mg S/(g VSS • h) until day 118, followed by a rapid increase to a level >20 mg S/(g VSS • h) with a maximum value of 38.6 mg S/(g VSS • h) achieved on day 129 (Fig. 1a). In SBR2, until day 103, SO_4^{2-} production was observed with the SPR in the range of 6.8–10 mg S/(g VSS • h). Subsequently, the S metabolism switched to utilization, a gradual increase in the SUR was observed from 1.5 to 10.6 mg S/(g VSS • h) until day 121 (Fig. 1b). After this period, similar to SBR1, there was a rapid increase in the SUR to a level >30 mg S/(g VSS • h) with a maximum value of 44.9 mg S/(g VSS • h) achieved on day 125. After day 120, SO_4^{2-} began to accumulate in both reactors, and the initial of SO_4^{2-} concentrations reached their highest values, fluctuating in the range of 1400–1600 mg S/L.

3.2. Sulfur-dependent autotrophic and heterotrophic denitrification indicators (NPR/NUR, CUR)

The dynamics of CUR and NPR/NUR throughout the entire study

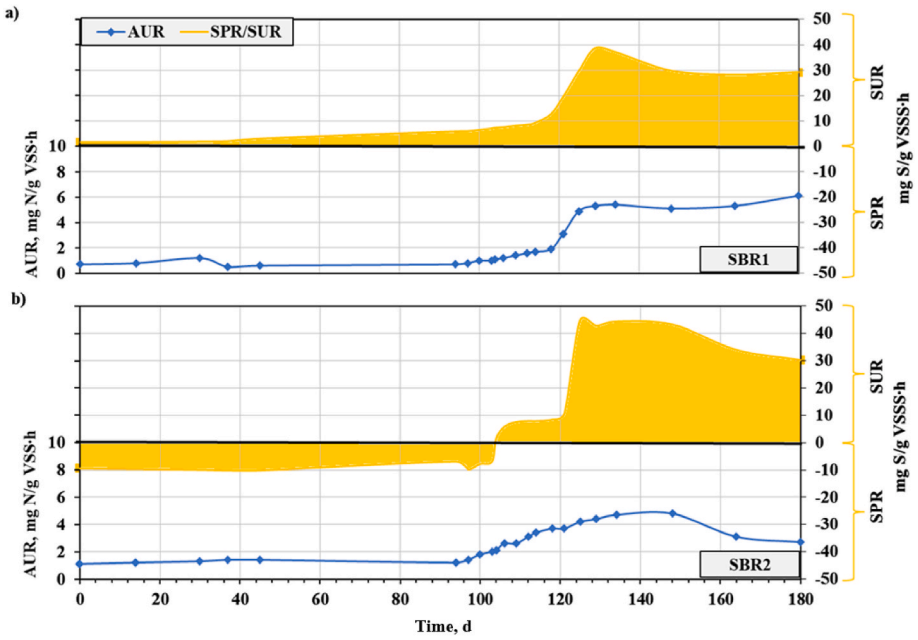

Fig. 1. The dynamics of AUR and SPR/SUR in SBR1 (a) and SBR2 (b).

period are presented in Fig. 2. In SBR1, initially (0–45 days), the NUR ranged from 0.2 to 0.6 mg N/(g VSS • h). Subsequently, the N metabolism switched to production, with the NPR ranging from 0.05 to 0.4 mg N/(g VSS • h) until the end of the study (Fig. 2a). In the contrary, in SBR2, only NO_3^- utilization was observed from the beginning of the study. The NURs increased from the initial level of approximately 1.2 mg N/(g VSS • h) to >2 mg N/(g VSS • h) after 30 days of operation and then remained relatively constant. The CURs were more variable during the study period and fluctuated in the range of 5.4–13.6 mg COD/(g VSS • h) (Fig. 2b).

3.3. *The efficiency of process utilization when combining the N–S/N–S–C cycles*

The efficiency of N utilization (NH_4^+, NO_3^- and TN) in both reactors is illustrated in Fig. 3a (SBR1) and Fig. 3b (SBR2). The efficiency was notably higher in SBR2, performing the N–S–C cycle, compared to SBR1, performing the N–S cycle. With the elevation of influent SO_4^{2-} concentration after day 100, NH_4^+ utilization efficiency increased, reaching a maximum of 64% and 100% almost in SBR1 and SBR2, respectively.

Regarding NO_3^- metabolism in SBR1, NO_3^- production switched to accumulation on day 100, reaching a maximum of 64% on day 129. In SBR2, NO_3^- utilization occurred throughout the entire experiment, with the efficiencies ranging from 54% to 100%. The efficiency of TN utilization, involving the change in the sum of NH_4^+ and NO_3^- concentrations, reached a maximum of 57% and almost 100% in SBR1 and SBR2, respectively.

The efficiency of SO_4^{2-} and COD utilization/production are presented in Fig. 4. The efficiency of SO_4^{2-} utilization in SBR1 ranged from 3% to 31% with the maximum value on day 104. In contrast, in SBR2, initially SO_4^{2-} was produced and then utilized from day 104, reaching a maximum (40%) on day 125. Meanwhile, the efficiency of COD utilization in SBR2 ranged from 40% to 66%, with the maximum value on day 118.

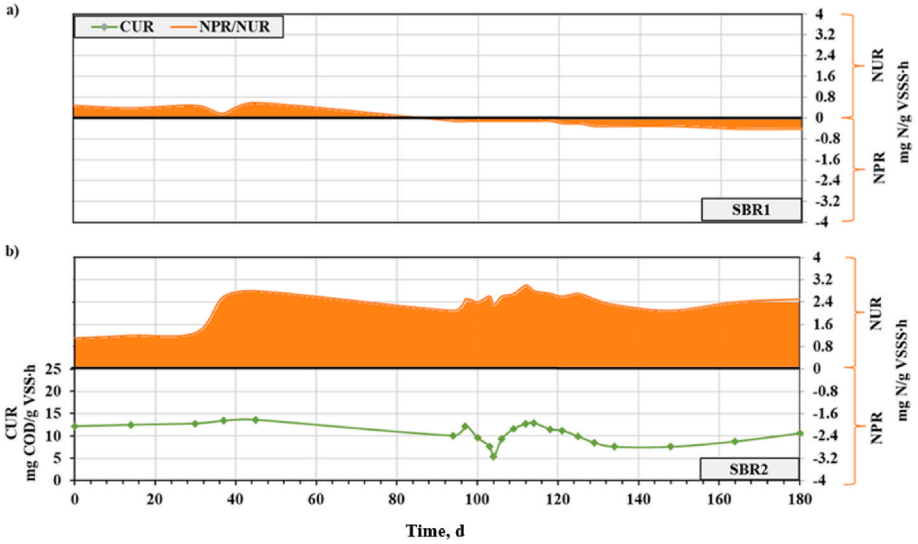

Fig. 2. The dynamics of NPR/NUR and CUR in SBR1 (a) and SBR2 (b).

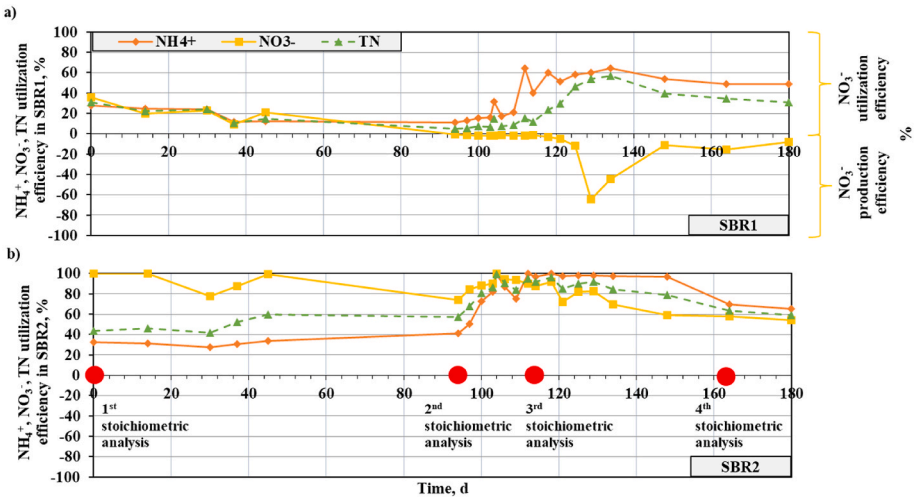

Fig. 3. NH_4^+, NO_3^- and TN utilization efficiencies in SBR1 (a) and SBR2 (b).

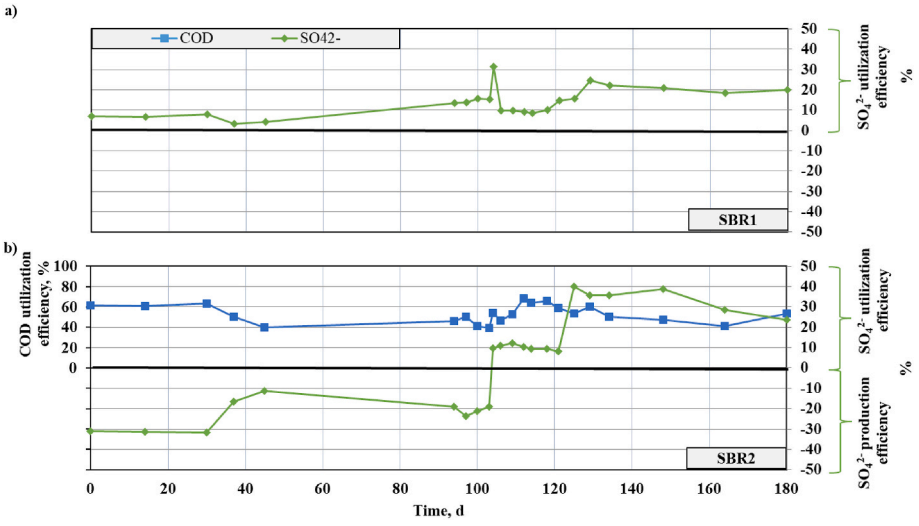

Fig. 4. SO_4^{2-} and COD utilization efficiencies in SBR1 (a) and SBR2 (b).

3.4. Stoichiometric calculations

The days selected for stoichiometric analysis (1 d, 94 d, 114 d, 164 d) are presented in Fig. 3. Figs. 5 and 6 illustrate the results of the analysis in the form of Sankey diagrams for the days prior to starting the supplementation of SO_4^{2-} (day 94) and after stabilizing the supplementation (day 164). For further comparison, the results of stoichiometric calculations on days 1 and 114 are shown in Fig. S4. In general, in SBR1, the reactions were primarily associated with anammox, SRAO, and other SO_4^{2-} utilization pathways, with a minor contribution from SDAD. On the other hand, SBR2 involved SRAO, mixotrophic denitrification, and other SO_4^{2-} utilization pathways.

Specifically, in SBR1, the AURs related to SRAO were 0.51 mg N/(g VSS • h) and 3.84 mg N/(g VSS • h) on days 94 and 164, respectively. Concurrently, on the same days, the AURs related to anammox were 0.19 mg N/(g VSS • h) and 1.46 mg N/(g VSS • h). Notably, both AURs exhibited an approximately 7.5-fold increase following the SO_4^{2-} supplementation. It should be emphasized that the AUR related to anammox became evident only after triggering NO_2^- production by SRAO. The NO_2^- generated from SRAO served as a substrate for the activation of anammox, leading to a rise in NiUR_amx from 0.25 mg N/(g VSS • h) to 1.92 mg N/(g VSS • h). This, in turn, influenced the NPR from anammox, increasing from 0.05 mg N/(g VSS • h) to 0.38 mg N/(g VSS • h).

Fig. 5a–b explicitly shows that the S transformations in SBR1 primarily concentrated on the reduction of SO_4^{2-}, while the SPR remained close to 0. The SUR in SBR1 related to both SRAO and non N-related processes (SUR_other). The SUR from SRAO raised from 0.87 mg S/(g VSS • h) to 6.57 mg S/(g VSS • h) between days 94 and 164, while the SUR_other increased from 5.03 mg S/(g VSS • h) to 21.73 mg S/(g VSS • H) during the same period. The SPR remained close to 0 mg S/(g VSS • h).

The results of the analysis for SBR2 (Fig. 6a–b) revealed a gradual prevalence of SRAO and mixotrophic denitrification in the expense of anammox, which completely disappeared at the end of the study period. The AUR related to SRAO increased from 0.05 mg N/(g VSS • h) to 3.1 mg N/(g VSS • h), whereas the AUR related to anammox decreased from 1.14 mg N/(g VSS • h) to 0 mg N/(g VSS • h) between days 94 and 164. Consequently, the contribution of NiUR and NPR from anammox also diminished to 0 mg N/(g VSS • h). Fig. 6b explicitly demonstrates the absence of anammox activity in the final phase of the study. On day 94, the NUR was facilitated by SDAD (2.4 mg N/(g VSS • h)), succeeded by NiUR through heterotrophic denitrification (0.91 mg N/(g VSS • h)). Conversely, on day 164, the dynamics of N transformations shifted (Fig. 6b), with the NUR related to heterotrophic denitrification (2.4 mg N/(g VSS • h)) and NiUR related to SDAD (3.95 mg N/(g VSS • h)).

On day 94, primarily SPR_other occurred alongside SPR in SDAD

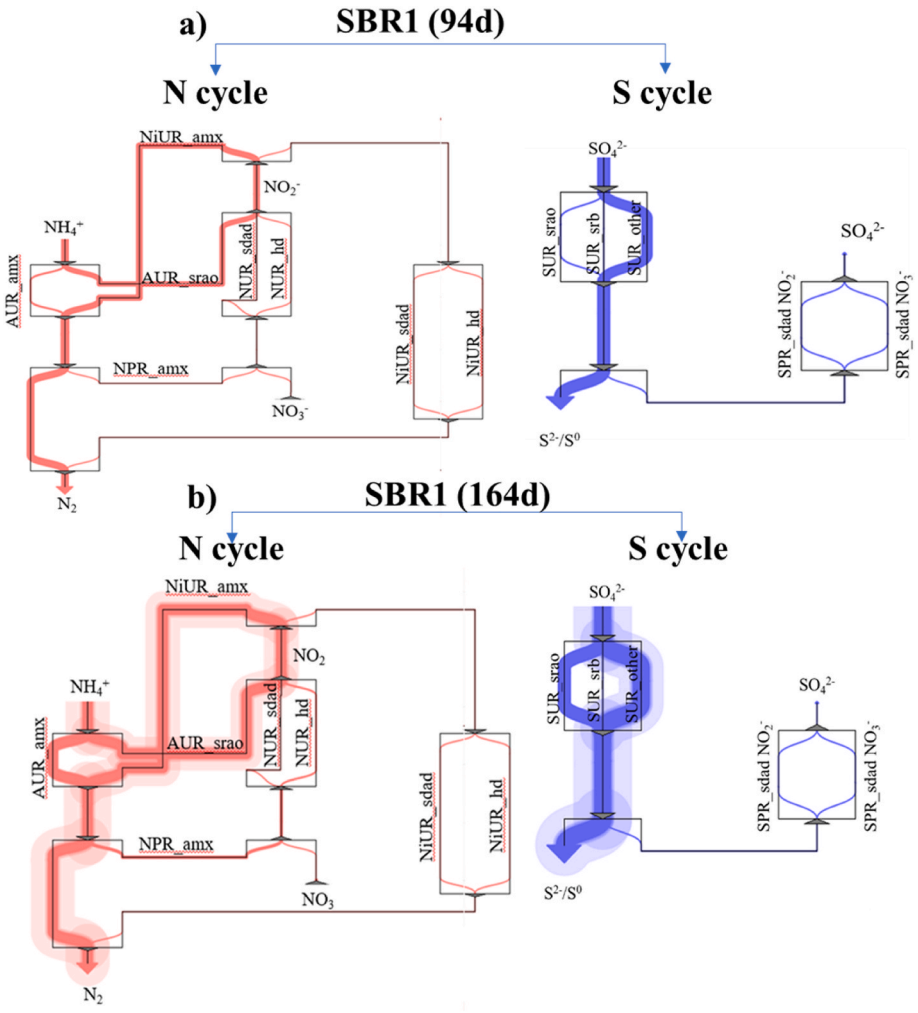

Fig. 5. Results of stoichiometric analysis in SBR1 on day 94 (a) and 164 (b).

involving NO_3^-. The SUR was lower and primarily attributed to SRB. On day 164, mainly SUR_other occurred, surging to 32 mg S/(g VSS • h), with the SUR from SRAO exceeding 5.3 mg S/(g VSS • h). The SO_4^{2-} production was mainly due to SDAD involving NO_2^-. Fig. 6a–b illustrates that the S transformations in SBR2 primarily focused on production on day 94 and the reduction of SO_4^{2-} on day 164.

The CUR in SBR2 related to both SRB activity and mixotrophic denitrification. Towards the end of the study, the SRB contribution diminished, and CUR primarily resulted from heterotrophic denitrification with NO_3^-, as shown in Fig. 6b. The influence of COD on the N–S–C transformations is evident when comparing SBR1 and SBR2 on the same days (i.e., 94 and 164). On day 94, SBR2 exhibited a 10-fold lower AUR_srao and a 6-fold higher AUR_amx compared to SBR1. Conversely, on day 164, SBR2 displayed a 1.2-fold lower AUR_srao and a complete halting AUR_amx, contrasting with SBR1. Additionally, SBR2 demonstrated mixotrophic denitrification, which was absent in SBR1 on days 94 and 164.

When comparing the S transformations in both reactors, different metabolic pathways were explicitly observed on day 94. A net reduction of SO_4^{2-} was observed in SBR1, while SBR2 experienced a net production of SO_4^{2-}. Specifically, in SBR1, the predominant process was SUR_other, whereas in SBR2, the S transformations involved SPR_other and SUR_srb. On the contrary, on day 164, both reactors mainly exhibited SUR_srao and SUR_other, however, a notable distinction was observed in SBR2, where SPR_niur from SDAD also contributed to the S transformations.

3.5. Microbiology

The bacterial community was analyzed using sequences of 16S rRNA gene amplicon. The average number of reads in samples representing SBR1 was 72,010. In the case of SBR2, the average number of reads was 61952,25. The Good's coverage values were 99.6% for both reactors. The average OTUs numbers in SBR1 was 114,00, whereas in SBR2 average OTUs number was 999. The average value of the Shannon diversity index was 4.51 for SBR1 and 4.46 for SBR2. The PERMANOVA test showed a lack of significant differences between the microbial community structures representing the studied reactors ($p = 0.752$).

At the phylum level, in SBR 1, the most abundant bacteria belonged to *Chloroflexi* (26.44%), *Proteobacteria* (19.67%), *Bacteroidota* (16.81%), and *Planctomycetota* (14.06%). Similarly, in SBR2, the most abundant phyla were *Chloroflexi* (23.61%), *Proteobacteria* (23.00%), *Bacteroidota* (17.84%), and *Planctomycetota* (14.79%) (Fig. 7). Less common were the phyla *Actinobacteriota* and *Acidobacteriota*, with abundance of 9.19% and 5.43) in SBR1, and 7.89 and 5.05, respectively. Bacteria from other phyla accounted for less than 2% of all bacteria.

At the genus level, the most numerous genera were generally *Candidatus* Brocadia and PHOS-HE36 (*Ignavibacteriales*), with average abundances of 7.73% and 7.95% in SBR1, and 9.38% and 7.89 in SBR2, respectively. A relatively abundant genus was AKYH767 (*Sphingobacteriales*), accounting for 5.45% in SBR1 and 6.02% in SBR2. Common in both reactors were three genera from the *Anaerolineaceae* family (SBR1031, RBG-13-54-9, and one uncultured genus), together

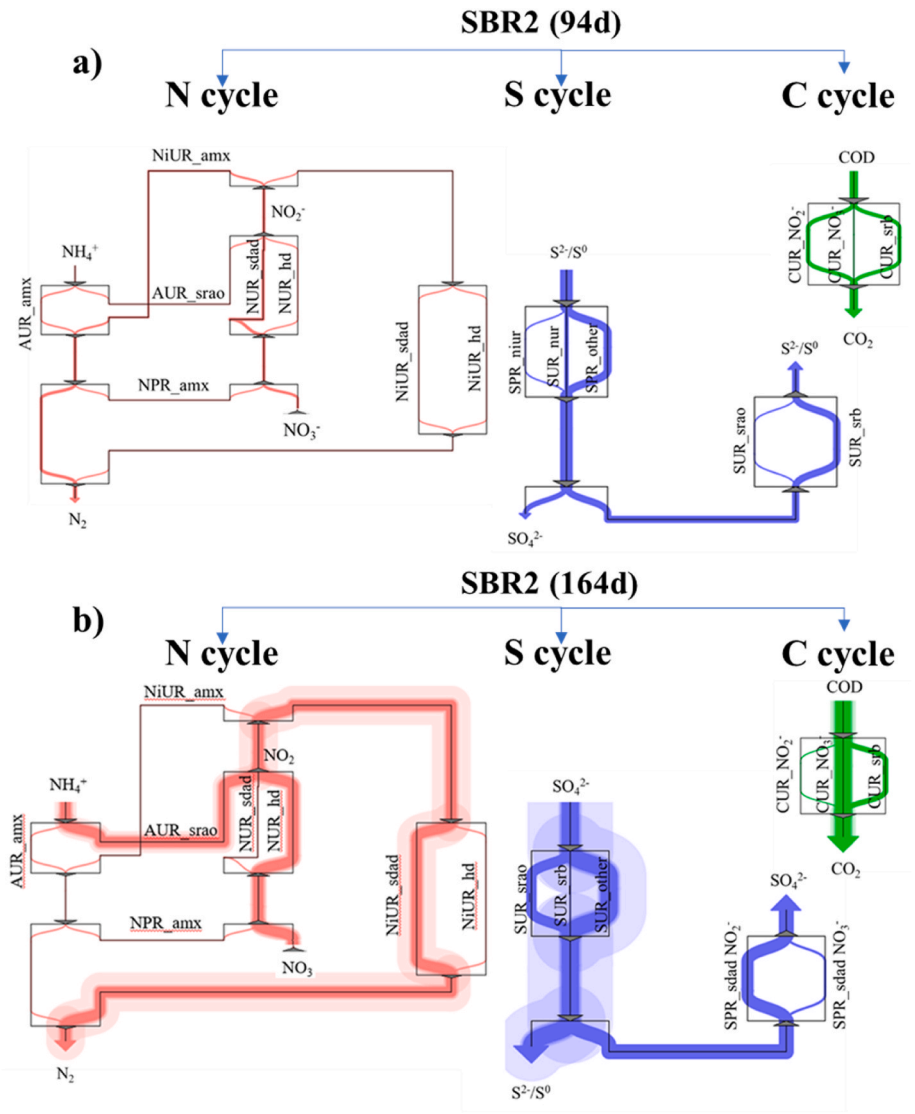

Fig. 6. Results of stoichiometric analysis in SBR2 on day 94 (a) and 164 (b).

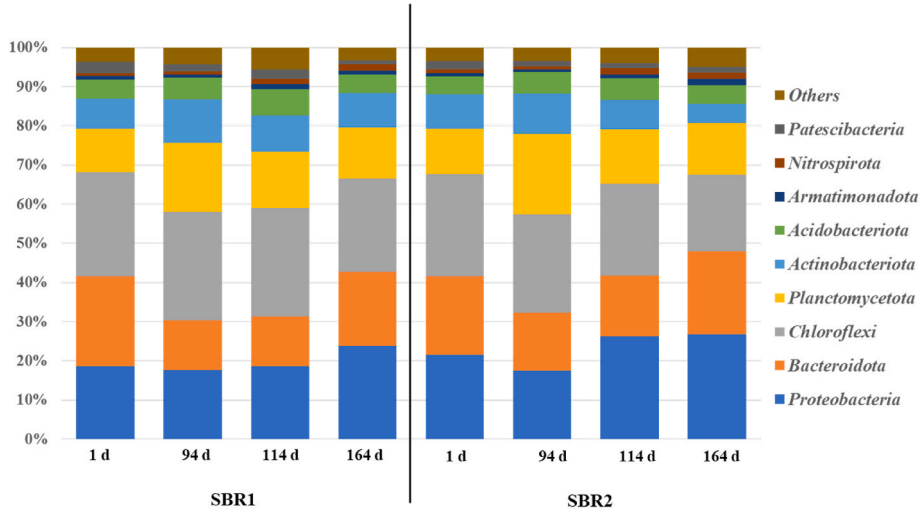

Fig. 7. Relative abundance of bacteria at the phylum level on days 1, 94, 114, and 164 in SBR1 and SBR2.

accounting for 5.83% and 5.21% in SBR1 and SBR2, respectively. Bacteria from *Burkholderiales* (*Thauera*, *Denitratisoma*, B1–7BS, *Limnobacter*) constituted another significant group in both reactors (Fig. S5). Among them, *Thauera* sp. and *Denitratisoma* sp. were more common in SBR2.

The phylogenetic tree, developed based on the genetic distance between samples, shows changes in the microbial community structure during process performance (Fig. S6). Samples from both reactors were very similar on the first day and formed a separate clade. The second group was formed by samples collected from both reactors on day 94 and one sample collected from SBR1 on day 114. The final group consisted of a sample collected from SBR2 on day 114 and samples collected from both reactors on day 164. The tree showed that changes in microbial communities began after 114 days in SBR1 and 94 days in SBR2.

4. Discussion

4.1. Current insights into coupling of N–S–C cycles in wastewater treatment

The utilization of SO_4^{2-} alongside NH_4^+ has garnered increasing attention in wastewater treatment due to its potential to enhance N utilization efficiencies. Existing literature, e.g., Fdz-Polanco et al. (2001) and Liu et al. (2008), has highlighted SO_4^{2-} role as an additional electron acceptor for anaerobic NH_4^+ oxidation, augmenting NH_4^+ utilization processes. Liu et al. (2008) observed an NH_4^+/NO_2^- consumption ratio of approximately 1.1:1 when $(NH_4)_2SO_4$ was present in the influent, surpassing a theoretical value of 1:1.34, indicating the significant impact of SO_4^{2-} on NH_4^+ utilization. Yang et al. (2009) and Zhang et al. (2019) demonstrated the synergistic effect of elevated NH_4^+ and SO_4^{2-} concentrations, leading to improved utilization efficiencies for both compounds. For instance, Zhang et al. (2019) observed that increasing influent SO_4^{2-} concentrations from approximately 100 mg S/L to 180 mg S/L, along with higher NH_4^+ concentrations (50 mg N/L vs. 120 mg N/L), improved NH_4^+ utilization efficiency from approximately 40%–90%. Wu et al. (2020) reported remarkable success in achieving an NH_4^+ utilization efficiency of 98%, including 44% removed through sulfammox (SRAO). Moreover, the presence of COD significantly impacts the anammox/mixotrophic denitrification process. Wang et al. (2016) illustrated the dominance of autotrophic AnAOB in low COD environments, while denitrifying heterotrophs thrived in higher COD environments. The coupling of anammox with SDAD can occur in two alternative pathways. When NO_3^- is present in the wastewater, anammox bacteria utilize the NO_2^- generated during partial SDAD, as described by Ma et al. (2022b). The second pathway involves producing NO_3^- through anammox for further denitrification, as in our previous studies (Derwis et al., 2023, 2024).

Studies by Qian et al. (2015) and Du et al. (2020) emphasized the significant impact of COD on denitrification processes, with mixotrophic denitrification showing higher TN utilization efficiencies compared to SDAD alone. Qian et al. (2015) observed a rapid increase in the rate of mixotrophic denitrification when COD was added to the SDAD reactor, approximately 10 times faster compared to studies without COD (Lee et al., 2001; Kim et al., 2002). Furthermore, Du et al. (2020) reported an increase in TN utilization efficiency from 70% in SDAD to 97% in mixotrophic denitrification. Wang et al. (2020) also suggested that SDAD can be applied in the treatment of low C/N wastewater, integrating different biological N removal processes (e.g., anammox) and facilitating the removal of multiple components.

4.2. Balancing autotrophic and mixotrophic conditions for improved NH_4^+ oxidation, SO_4^{2-} utilization and wastewater treatment efficiency

The results of this study reveal significant insights into the impact of various factors on the treatment processes within the reactors. Increasing the SO_4^{2-} influent after day 100 led to an increase in both AUR and SUR in both reactors. Notably, the SO_4^{2-} influent had a greater effect on AUR in SBR1, achieving a higher value compared to SBR2. In contrast, it had an inverse effect on SUR, yielding better results in SBR2. Thus, maintaining autotrophic conditions without COD addition is crucial for faster NH_4^+ oxidation, whereas for faster SO_4^{2-} utilization, mixotrophic conditions with COD addition, especially at high SO_4^{2-} concentrations (>300 mg S/L), appear to be more favorable. The efficiency of TN removal also increased in both reactors with increased SO_4^{2-} influent. In SBR2, at low SO_4^{2-} concentrations (<300 mg S/L), SO_4^{2-} production occurred initially, followed by effective SO_4^{2-} utilization after increasing the influent to >300 mg S/L.

The optimal initial N/S and N/S/C ratios were determined based on the observed TN and SO_4^{2-} utilization efficiencies. For SBR1, the most effective N/S ratio for TN utilization efficiency was found to be 1/16, and for SO_4^{2-} utilization efficiency - it was 1/3.5. In contrast, in SBR2, the optimal N/S/C ratio for TN utilization efficiency was identified as 1/16/2.8, while for SO_4^{2-} utilization efficiency - it was 1/24/2.8. In the case of wastewater loaded with NO_3^-, mixotrophic conditions seem to be more advantageous due to faster NO_3^- utilization in SBR2 compared to SBR1, where utilization eventually shifted to production under autotrophic conditions over time. Anammox surpassed SDAD in SBR1, whereas mixotrophic denitrification played a crucial role in SBR2, influencing higher NUR values. Overall, in SBR1, reactions were mainly associated with anammox, SRAO, and other SO_4^{2-} utilization pathways, with minimal SDAD involvement. Conversely, SBR2 involved SRAO, mixotrophic denitrification, and other SO_4^{2-} utilization pathways. In SBR1, both AUR from anammox and SRAO processes increased approximately 7.5 times after increasing SO_4^{2-} supplementation. Anammox utilized NO_2^- generated from the SRAO process, mutually enhancing NH_4^+ utilization efficiency. However, in SBR2, the SRAO process surpassed anammox after increasing SO_4^{2-} supplementation. This could be related to the addition of COD in SBR2, which adversely affected the anammox process, allowing SRAO to oxidize NH_4^+ under these conditions. Nevertheless, comparing AUR values for both processes at the end of the study, both SRAO and anammox processes exhibited lower AUR for SBR2 compared to SBR1. Therefore, for better NH_4^+ utilization results in anammox and SRAO processes, autotrophic conditions without COD are recommended. In both reactors, SRAO primarily accounted for SO_4^{2-} utilization, along with processes unrelated to the N cycle, with a minor additional contribution from SRB in SBR2.

These findings underscore the complexity of microbial interactions and the importance of understanding them for optimizing wastewater treatment processes. Moreover, they highlight the significance of research in elucidating these mechanisms and guiding efficient treatment strategies for environmental protection and resource recovery.

4.3. Impact of NO_2^- addition on N–S–C cycles under transformations

Our previous studies (Derwis et al., 2023, 2024) focused on the dynamics of N–S–C transformations, specifically exploring the impact of NO_2^- without concurrent NO_3^- addition under autotrophic (Derwis et al., 2023) and heterotrophic conditions (Derwis et al., 2024). The present study elucidated the differences and similarities arising from the absence of NO_2^- and the inclusion of NO_3^-.

In the study by Derwis et al. (2023) in the reactor receiving both SO_4^{2-} and NO_2^-, the study revealed the concurrent development of SRAO process, AOB, anammox and SDAD. SO_4^{2-} was primarily generated in SDAD through the involvement of NO_2^-. Processes independent of the N cycle also contributed significantly to SO_4^{2-} removal.

In contrast, the addition of SO_4^{2-} and NO_3^- in this study resulted in significantly slower process rates for SRAO (3 times) and anammox (17 times) compared to the autotrophic conditions studied by Derwis et al. (2023). Moreover, the SDAD process only developed to a minimal extent. Therefore, the addition of NO_2^- favored anaerobic NH_4^+ oxidation with SO_4^{2-} addition for both SRAO and anammox. SDAD also demonstrated better performance with the addition of NO_2^- than NO_3^-, indicating a preference of S-dependent autotrophic bacteria for NO_2^- in

oxidizing reduced S compounds.

Under heterotrophic conditions with the addition of SO_4^{2-}, COD and NO_2^- (Derwis et al., 2024), the development of SRAO, anammox, mixotrophic denitrification was observed. When NO_3^- was added instead of NO_2^- in the present study, SRAO developed to a similar extent, while anammox disappeared. Mixotrophic denitrification emerged, where NO_3^- and NO_2^- were primarily reduced by heterotrophs and S-dependent autotrophs, respectively, aligning with the findings of Derwis et al. (2024). One of the key findings was that anammox thrived under COD conditions, but the presence of NO_2^- was essential. In the absence of NO_2^- under heterotrophic conditions, anammox disappeared.

4.4. Microbial community dynamics and functional roles in S-based systems

Taxonomic analyses revealed that the microbial communities were predominantly composed of members from the genera *Candidatus* Brocadia and PHOS -HE36 with the average abundances in both reactors of 8.55% and 7.92%, respectively. While the former taxon is commonly known as conventional anammox bacteria, it could potentially be responsible for performing the entire SRAO reaction (Liu et al., 2015; Grubba et al., 2021). The role of PHOS -HE36 remains less understood, but it was identified as the dominant bacterium (9.59%) in a system performing S-based autotrophic denitrification (Fu et al., 2023). It has also been speculated that these obligate heterotrophic bacteria might be involved in the denitrification process (Koenig et al., 2005; Fu et al., 2023).

The hypothesis suggested PHOS -HE36's role as a symbiotic provider of necessary NO_2^- to *Candidatus* Brocadia. However, results reveal no significant correlation despite the relatively high frequency of both types. The complexity of the symbiosis, potentially heightened by the presence of numerous denitrifiers, may account for this observation. The current challenge lies in discerning whether alternative metabolic pathways might influence this association.

Other dominant genera, such as AKYH767 (average abundance of 5.73% in both reactors 5.73%) and SBR1031 (average abundance of 5.34% in both reactors), were common. Notably, all three genera (PHOS -HE36, AKYH767, and SBR1031) were also found in similar abundances by Fu et al. (2023). AKYH767 likely belongs to aerobic organotrophs (Kim et al., 2020), while SBR1031 belongs to anaerobic bacteria capable of fermenting carbohydrates, and its metabolic function is related to NH_4^+ conversion (Wang et al., 2018; Sun et al., 2020; Fu et al., 2023).

In the work of Hu et al. (2022), investigating a Feammox-based process, PHOS-HE36 (7.13%), SBR1031 (4.41%), and *Denitratisoma* (5.06%) were found in the seed anammox sludge. Following the process start-up, these genera enriched their abundances. The authors suggested that they all were heterotrophic denitrifiers and played a similar role in the Feammox bioreactor. In the present study, PLTA13 (Ma et al., 2022a), *Limnobacter*, and uncultured bacteria from the *Anaerolineaceae* family were involved in heterotrophic denitrification, in addition to PHOS -HE36, SBR1031, *Denitratisoma*. In the work of Deng et al. (2024), the performance of N removal by PD/anammox process with Fe(II) addition was assessed. The authors identified *Denitratisoma*, Ignavibacterium, *Thauera* and *Limnobacter* as key genera providing NO_2^- substrate for the subsequent anammox reaction, primarily facilitated by *Candidatus* Brocadia. In our study, the abundance of *Thauera* was significantly higher in SBR2 than in SBR1 (Fig. S5). The substantial increase in *Thauera* abundance after 100 days suggests a potential correlation between its activity and the enhanced NH_4^+ utilization observed in SBR2.

In addition, members of the genus *Thauera* may be responsible for the reduction of SO_4^{2-} as an electron donor (Huang et al., 2015). Members of the B1–7BS family, with an average abundance of 3.65% in our reactors, have previously been retrieved from various environments, including an alpine cave (Jurado et al., 2020), an S^{2-} mineral deposit (Jones et al., 2017), and a lava tube cave (Gonzalez-Pimentel et al., 2021). Hence, it is reasonable to infer that these genera, along with *Thauera*, contribute to S utilization. Moreover, the oxidation of NH_4^+ utilizing SO_4^{2-} as an electron acceptor appears to be a multifaceted process that entails multiple sequential steps executed by a consortium of species.

4.5. Future perspectives and practical applications of S-dependent systems of anaerobic NH_4^+ oxidation combined with denitrification

Future perspectives of SO_4^{2-}-dependent systems in wastewater treatment encompass the continuous improvement and optimization of technologies that integrate SRAO in combination with SDAD/anammox (forming the N–S cycle) or mixotrophic denitrification/anammox (forming the N–S–C cycle). These systems exhibit high effectiveness in treating wastewater with elevated concentrations of NH_4^+, NO_3^-, SO_4^{2-} and COD, especially in scenarios with low NO_2^- content, i.e. those that can be used in the PD/anammox process, which is the first key insight. SO_4^{2-}-dependent systems demonstrate the effective removal of NH_4^+ by utilizing SO_4^{2-} in the case of lacking an electron acceptor for anammox in the form of NO_2^-, which is the second key insight. This resilience makes these systems versatile and reliable in a variety of applications to diverse wastewater compositions.

The integration of the S cycle plays a key role in SO_4^{2-}-dependent systems, serving as a driving force for N and C transformations, i.e. those present in PD/anammox, which is the third key insight. This complex N–S–C cycle involves the reduction of SO_4^{2-} in the SRAO process (N–S cycle) or by SRB (N–S–C cycle), and the subsequent re-oxidation of reduced S species in the SDAD process. In the presence of COD, mixotrophic denitrification becomes the dominant pathway of N transformations.

In the field of SO_4^{2-}-dependent anaerobic NH_4^+ oxidation systems combined with denitrification, an additional research direction involves interactions between the microbial groups. The complex interactions among microorganisms responsible for SRAO, SDAD and mixotrophic denitrification pose challenges for a comprehensive understanding, hindering the unlocking of the full potential of SO_4^{2-}-dependent systems, which is the fourth key insight. Further research efforts should focus on elucidating these microbial interactions to uncover hidden synergies, improve system performance and potentially discover untapped microbial functionalities.

Another study (Jia et al., 2017) explored the integration of N–S–C cycles through the Sulfate-reduction Autotrophic-denitrification and Nitrification Integrated (SANI). That process employs SO_4^{2-} as an electron acceptor for organic matter removal, while utilizing S^{2-} as an electron donor for N removal via autotrophic denitrification. This differs from our study, where SO_4^{2-} primarily enhances NH_4^+ utilization efficiency in SRAO and mixotrophic denitrification is responsible for COD reduction. Additionally, our approach does not involve oxygenation, thereby reducing operational costs.

In the study of Li et al. (2022), autotrophic-heterotrophic denitrification was investigated, emphasizing two primary biological pathways: simultaneous nitrification and denitrification (SNAD), and PD/anammox. SNAD operates in oxygen-limited environments, involving concurrent processes of nitrification, denitrification, and anammox. In contrast, PD/anammox pathways occur under anaerobic conditions, combining partial denitritation with anammox. Both pathways yield NO_2^- for anammox. However, our research indicates that NO_2^- is not essential for NH_4^+ oxidation, and the N–C cycles can be extended via the S cycle, where SO_4^{2-} serves as an adequate electron acceptor for NH_4^+. Furthermore, NO_2^- generated in SRAO can be utilized in anammox, enhancing NH_4^+ oxidation under anaerobic conditions.

In practical applications, SO_4^{2-}-dependent systems offer a sustainable and flexible solution for the treatment of complex wastewater. Ongoing studies should concentrate on improving the efficiency, cost-effectiveness, and environmental sustainability of SO_4^{2-}-dependent systems to make them integral components of future wastewater treatment strategies.

5. Conclusions

The study demonstrated the viability of integrating either SDAD or mixotrophic denitrification with the anammox process in a single reactor, specifically designed for treating streams rich in NH_4^+, NO_3^-, SO_4^{2-} and COD. It confirmed that SO_4^{2-} - dependent systems are capable of generating NO_2^- to facilitate NH_4^+ oxidation. Additionally, the SRAO process served as an extra electron acceptor for NH_4^+ oxidation while reducing SO_4^{2-} to produce S compounds for SDAD. Increasing the influent SO_4^{2-} concentrations enhanced the utilization rates and efficiencies of NH_4^+ and SO_4^{2-}. Optimal N/S and N/S/C ratios were determined to maximize TN and SO_4^{2-} utilization efficiencies in SBR1 and SBR2. Essential pathways included anammox, SRAO, and SO_4^{2-} utilization (SBR1) compared to SRAO, mixotrophic denitrification, and SO_4^{2-} production (SBR2). The study emphasized the capacity of anammox bacteria to maintain high activity and abundance within a microbial consortium over prolonged periods, contingent upon balanced concentrations of N, S and COD compounds. The SRAO process was likely facilitated by dominant genera, such as *Candidatus*_Brocadia and PHOS-HE36.

Funding

This work was supported by the Polish National Science Centre under the project no. 2020/37/N/ST8/02,455 and the Argentum project grant no: January 17, 2022/IDUB/I3b/Ag, 2022/2023.

CRediT authorship contribution statement

Dominika Derwis: Writing – original draft, Visualization, Project administration, Investigation, Funding acquisition, Formal analysis, Conceptualization. **Hussein E. Al-Hazmi:** Writing – original draft, Visualization, Methodology, Investigation. **Joanna Majtacz:** Visualization, Methodology, Investigation, Formal analysis, Conceptualization. **Sławomir Ciesielski:** Writing – original draft. **Jacek Mąkinia:** Writing – review & editing, Validation, Supervision.

Declaration of competing interest

The authors declare that they have no known competing financial interests or personal relationships that could have appeared to influence the work reported in this paper.

Data availability

Data will be made available on request.

Appendix A. Supplementary data

Supplementary data to this article can be found online at https://doi.org/10.1016/j.jenvman.2024.120908.

References

Al-Hazmi, H.E., Lu, X., Majtacz, J., Kowal, P., Xie, L., Makinia, J., 2020. Optimization of the aeration strategies in a deammonification sequencing batch reactor for efficient nitrogen removal and mitigation of N2O production. Environ. Sci. Technol. https://doi.org/10.1021/acs.est.0c04229.

Al-Hazmi, H.E., Maktabifard, M., Grubba, D., Majtacz, J., Hassan, G.K., Lu, X., Piechota, G., Mannina, G., Bott, C.B., Mąkinia, J., 2023. An advanced synergy of partial denitrification-anammox for optimizing nitrogen removal from wastewater: a review. Bioresour. Technol., 129168 https://doi.org/10.1016/j.biortech.2023.129168.

Cao, S., Du, R., Peng, Y., Li, B., Wang, S., 2019. Novel two stage partial denitrification (PD)-Anammox process for tertiary nitrogen removal from low carbon/nitrogen (C/N) municipal sewage. Chem. Eng. J. 362, 107–115. https://doi.org/10.1016/j.cej.2018.12.160.

Deng, Z., Chen, Y., Zhang, C., Chen, Z., Li, Y., Huang, L., Wang, Z., Wang, X., 2024. Improving nitrogen removal performance from rare earth wastewater via partial denitrification and anammox process with Fe(II) amendment. J. Water Proc. Eng. 60, 105131 https://doi.org/10.1016/j.jwpe.2024.105131.

Derwis, D., Al-Hazmi, H.E., Majtacz, J., Kowal, P., Ciesielski, S., Mąkinia, J., 2024. The role of the combined nitrogen-sulfur-carbon cycles for efficient performance of anammox-based systems. Sci. Total Environ. 917, 170477 https://doi.org/10.1016/j.scitotenv.2024.170477.

Derwis, D., Majtacz, J., Kowal, P., Al-Hazmi, H.E., Zhai, J., Ciesielski, S., Piechota, G., Mąkinia, J., 2023. Integration of the sulfate reduction and anammox processes for enhancing sustainable nitrogen removal in granular sludge reactors. Bioresour. Technol. 383, 129264 https://doi.org/10.1016/j.biortech.2023.129264.

Di Capua, F., Pirozzi, F., Lens, P.N.L., Esposito, G., 2019. Electron donors for autotrophic denitrification. Chem. Eng. J. 362, 922–937. https://doi.org/10.1016/j.cej.2019.01.069.

Du, S., Ya, T., Zhang, M., Zhu, M., Li, N., Liu, S., Wang, X., 2020. Distinct microbial communities and their networks in an anammox coupled with sulfur autotrophic/mixotrophic denitrification system. Environ. Pollut. 262, 114190 https://doi.org/10.1016/j.envpol.2020.114190.

Fdz-Polanco, F., 2001. New process for simultaneous removal of nitrogen and sulphur under anaerobic conditions. Water Res. 35 (4), 1111–1114. https://doi.org/10.1016/s0043-1354(00)00474-7.

Fu, K., Zeng, Z., Huang, S., 2023. Effect of sulfur autotrophic denitrification sludge on the start-up characteristics of anaerobic ammonia oxidation. Water 15 (7), 1275. https://doi.org/10.3390/w15071275.

Gonzalez-Pimentel, J.L., Martin-Pozas, T., Jurado, V., Miller, A.Z., Caldeira, A.T., Fernandez-Lorenzo, O., Sanchez-Moral, S., Saiz-Jimenez, C., 2021. Prokaryotic communities from a lava tube cave in La Palma Island (Spain) are involved in the biogeochemical cycle of major elements. PeerJ 9, e11386. https://doi.org/10.7717/peerj.11386. Artykuł.

Greenberg, A.E., Clesceri, L.S., Eaton, A.D., 2005. APHA Standard methods for the examination of water and waste water. In: American Public Health Association, American Water Works Association, twenty-first ed. Water Pollution Control Federation, Washington, DC, USA.

Grubba, D., Majtacz, J., Mąkinia, J., 2021. Sulfate reducing ammonium oxidation (SULFAMMOX) process under anaerobic conditions. Environ. Technol. Innovat. 22, 101416 https://doi.org/10.1016/j.eti.2021.101416.

Grubba, D., Yin, Z., Majtacz, J., Al-Hazmi, H.E., Mąkinia, J., 2022. Incorporation of the sulfur cycle in sustainable nitrogen removal systems - a review. J. Clean. Prod. 133495 https://doi.org/10.1016/j.jclepro.2022.133495.

Hu, L., Cheng, X., Qi, G., Zheng, M., Dang, Y., Li, J., Xu, K., 2022. Achieving ammonium removal through anammox-derived Feammox with low demand of Fe(III). Front. Microbiol. 13 https://doi.org/10.3389/fmicb.2022.918634.

Huang, C., Zhao, Y., Li, Z., Yuan, Y., Chen, C., Tan, W., Gao, S., Gao, L., Zhou, J., Wang, A., 2015. Enhanced elementary sulfur recovery with sequential sulfate-reducing, denitrifying sulfide-oxidizing processes in a cylindrical-type anaerobic baffled reactor. Bioresour. Technol. 192, 478–485. https://doi.org/10.1016/j.biortech.2015.04.103.

Huang, S., Zheng, Z., Wei, Q., Han, I., Jaffé, P.R., 2019. Performance of sulfur-based autotrophic denitrification and denitrifiers for wastewater treatment under acidic conditions. Bioresour. Technol. 294, 122176 https://doi.org/10.1016/j.biortech.2019.122176.

Huang, X., Mi, W., Chan, Y.H., Singh, S., Zhuang, H., Leu, S.-Y., Li, X.-z., Li, X., Lee, P.-H., 2022. C-N-S synergy in a pilot-scale mainstream anammox fluidized-bed membrane bioreactor for treating chemically enhanced primary treatment saline sewage. Water Res. 119475 https://doi.org/10.1016/j.watres.2022.119475.

Jia, Y., Khanal, S.K., Zhang, H., Chen, G.-H., Lu, H., 2017. Sulfamethoxazole degradation in anaerobic sulfate-reducing bacteria sludge system. Water Res. 119, 12–20. https://doi.org/10.1016/j.watres.2017.04.040.

Jones, D.S., Lapakko, K.A., Wenz, Z.J., Olson, M.C., Roepke, E.W., Sadowsky, M.J., Novak, P.J., Bailey, J.V., 2017. Novel microbial assemblages dominate weathered sulfide-bearing rock from copper-nickel deposits in the duluth complex, Minnesota, USA. Appl. Environ. Microbiol. 83 (16) https://doi.org/10.1128/aem.00909-17.

Jurado, V., Gonzalez-Pimentel, J.L., Miller, A.Z., Hermosin, B., D'Angeli, I.M., Tognini, P., De Waele, J., Saiz-Jimenez, C., 2020. Microbial communities in vermiculation deposits from an alpine cave. Front. Earth Sci. 8 https://doi.org/10.3389/feart.2020.586248.

Kim, I., Oh, S., Bum, M., Lee, J., Lee, S., 2002. Monitoring the denitrification of wastewater containing high concentrations of nitrate with methanol in a sulfur-packed reactor. Appl. Microbiol. Biotechnol. 59 (1), 91–96. https://doi.org/10.1007/s00253-002-0952-5.

Kim, N., Zabaloy, M.C., Riggins, C.W., Rodríguez-Zas, S., Villamil, M.B., 2020. Microbial shifts following five years of cover cropping and tillage practices in fertile agroecosystems. Microorganisms 8 (11), 1773. https://doi.org/10.3390/microorganisms8111773.

Koenig, A., Zhang, T., Liu, L.-H., Fang, H.H.P., 2005. Microbial community and biochemistry process in autosulfurotrophic denitrifying biofilm. Chemosphere 58 (8), 1041–1047. https://doi.org/10.1016/j.chemosphere.2004.09.040.

Lee, D.-U., Lee, I.-S., Choi, Y.-D., Bae, J.-H., 2001. Effects of external carbon source and empty bed contact time on simultaneous heterotrophic and sulfur-utilizing autotrophic denitrification. Process Biochem. 36 (12), 1215–1224. https://doi.org/10.1016/s0032-9592(01)00163-7.

Li, J., Tabassum, S., 2022. Simultaneous removal of ammonia nitrogen and sulfide by coupled anammox and sulfur autotrophic denitrification process from industrial wastewater. Cleaner Eng. Technol. 8, 100469 https://doi.org/10.1016/j.clet.2022.100469.

Li, J., Peng, Y., Yang, S., Li, S., Feng, W., Li, X., Zhang, Q., Zhang, L., 2022. Successful application of anammox using the hybrid autotrophic–heterotrophic denitrification

process for low-strength wastewater treatment. Environ. Sci. Technol. https://doi.org/10.1021/acs.est.2c02920.
Liu, Z.C., Yuan, L.J., Zhou, G.B., Li, J., 2015. Achievement of sulfate-reducing anaerobic ammonium oxidation reactor started with nitrate-reducting anaerobic ammonium oxidation. Huanjing Kexue 36 (9), 3345–3351. Chinese. PMID: 26717697.
Liu, S., Yang, F., Gong, Z., Meng, F., Chen, H., Xue, Y., Furukawa, K., 2008. Application of anaerobic ammonium-oxidizing consortium to achieve completely autotrophic ammonium and sulfate removal. Bioresour. Technol. 99 (15), 6817–6825. https://doi.org/10.1016/j.biortech.2008.01.054.
Ma, J., Liu, H., Dang, H., Wu, X., Yan, Y., Zeng, T., Li, W., Chen, Y., 2022b. Realization of nitrite accumulation in an autotrophic-heterotrophic denitrification system using different S/N/C ratios coupled with ANAMMOX to achieve nitrogen removal. J. Chem. Technol. Biotechnol. https://doi.org/10.1002/jctb.7244.
Ma, J., Wang, K., Shi, C., Liu, Y., Yu, C., Fang, K., Fu, X., Yuan, Q., Zhou, Y., Gong, H., 2022a. A novel anammox aggregate nourished sustainably internal heterotrophic nitrate removal pathway with endogenous carbon source. Bioresour. Technol. 346, 126525 https://doi.org/10.1016/j.biortech.2021.126525.
Qian, J., Liu, R., Wei, L., Lu, H., Chen, G.-H., 2015. System evaluation and microbial analysis of a sulfur cycle-based wastewater treatment process for Co-treatment of simple wet flue gas desulfurization wastes with freshwater sewage. Water Res. 80, 189–199. https://doi.org/10.1016/j.watres.2015.05.005.
Qian, J., Zhang, M., Wu, Y., Niu, J., Chang, X., Yao, H., Hu, S., Pei, X., 2018. A feasibility study on biological nitrogen removal (BNR) via integrated thiosulfate-driven denitratation with anammox. Chemosphere 208, 793–799. https://doi.org/10.1016/j.chemosphere.2018.06.060.
Sun, H., Zhou, Q., Zhao, L., Wu, W., 2020. Enhanced simultaneous removal of nitrate and phosphate using novel solid carbon source/zero-valent iron composite. J. Clean. Prod. 125757 https://doi.org/10.1016/j.jclepro.2020.125757.
Sun, R., Zhang, L., Zhang, Z., Chen, G.-H., Jiang, F., 2018. Realizing high-rate sulfur reduction under sulfate-rich conditions in a biological sulfide production system to treat metal-laden wastewater deficient in organic matter. Water Res. 131, 239–245. https://doi.org/10.1016/j.watres.2017.12.039.
Wang, B., Peng, Y., Guo, Y., Yuan, Y., Zhao, M., Wang, S., 2016. Impact of partial nitritation degree and C/N ratio on simultaneous Sludge Fermentation, Denitrification and Anammox process. Bioresour. Technol. 219, 411–419. https://doi.org/10.1016/j.biortech.2016.07.114.
Wang, J.-J., Huang, B.-C., Li, J., Jin, R.-C., 2020. Advances and challenges of sulfur-driven autotrophic denitrification (SDAD) for nitrogen removal. Chin. Chem. Lett. 31 (10), 2567–2574. https://doi.org/10.1016/j.cclet.2020.07.036.
Wang, X., Yan, Y., Gao, D., 2018. The threshold of influent ammonium concentration for nitrate over-accumulation in a one-stage deammonification system with granular sludge without aeration. Sci. Total Environ. 634, 843–852. https://doi.org/10.1016/j.scitotenv.2018.04.053.
Wu, L., Yan, Z., Li, J., Huang, S., Li, Z., Shen, M., Peng, Y., 2020. Low temperature advanced nitrogen and sulfate removal from landfill leachate by nitrite-anammox and sulfate-anammox. Environ. Pollut. 259, 113763 https://doi.org/10.1016/j.envpol.2019.113763.
Wu, P., Chen, J., Kumar Garlapati, V., Zhang, X., Wani Victor Jenario, F., Li, X., Liu, W., Chen, C., Aminabhavi, T.M., Zhang, X., 2022. Novel insights into anammox-based processes: a critical review. Chem. Eng. J., 136534 https://doi.org/10.1016/j.cej.2022.136534.
Xu, G., Peng, J., Feng, C., Fang, F., Chen, S., Xu, Y., Wang, X., 2015. Evaluation of simultaneous autotrophic and heterotrophic denitrification processes and bacterial community structure analysis. Appl. Microbiol. Biotechnol. 99 (15), 6527–6536. https://doi.org/10.1007/s00253-015-6532-2.
Yang, Z., Zhou, S., Sun, Y., 2009. Start-up of simultaneous removal of ammonium and sulfate from an anaerobic ammonium oxidation (anammox) process in an anaerobic up-flow bioreactor. J. Hazard Mater. 169 (1–3), 113–118. https://doi.org/10.1016/j.jhazmat.2009.03.067.
Zekker, I., Rikmann, E., Oja, J., Anslan, S., Borzyszkowska, A.F., Zielińska-Jurek, A., Kumar, R., Shah, L.A., Naeem, M., Zahoor, M., Setyobudi, R.H., Bhowmick, G.D., Khattak, R., Burlakovs, J., Tenno, T., 2023. The selective salinity and hydrazine parameters for the start-up of non-anammox-specific biomass SBR. Int. J. Environ. Sci. Technol. https://doi.org/10.1007/s13762-023-05055-9.
Zekker, I., Rikmann, E., Tenno, T., Loorits, L., Kroon, K., Fritze, H., Tuomivirta, T., Vabamäe, P., Raudkivi, M., Mandel, A., Dc Rubin, S.S.C., Tenno, T., 2015. Nitric oxide for anammox recovery in a nitrite-inhibited deammonification system. Environ. Technol. 36 (19), 2477–2487. https://doi.org/10.1080/09593330.2015.1034791.
Zhang, D., Cui, L., Wang, H., Liang, J., 2019. Study of sulfate-reducing ammonium oxidation process and its microbial community composition. Water Sci. Technol. 79 (1), 137–144. https://doi.org/10.2166/wst.2019.027.
Zhang, Q., Xu, X., Zhang, R., Shao, B., Fan, K., Zhao, L., Ji, X., Ren, N., Lee, D.-J., Chen, C., 2022. The mixed/mixotrophic nitrogen removal for the effective and sustainable treatment of wastewater: from treatment process to microbial mechanism. Water Res. 226, 119269 https://doi.org/10.1016/j.watres.2022.119269.
Zhou, X., Song, J., Wang, G., Yin, Z., Cao, X., Gao, J., 2020. Unravelling nitrogen removal and nitrous oxide emission from mainstream integrated nitrification-partial denitrification-anammox for low carbon/nitrogen domestic wastewater. J. Environ. Manag. 270, 110872 https://doi.org/10.1016/j.jenvman.2020.110872.